




# Echocardiography of the right heart in pulmonary arterial hypertension: insights from the ULTRA RIGHT VALUE study

Francesco Lo Giudice<sup>1</sup>, Pilar Escribano-Subias<sup>2</sup>, Khodr Tello<sup>3</sup>, Grzegorz Kopec<sup>4</sup>, Stefano Ghio <sup>5</sup>, George Giannakoulas<sup>6</sup>, Michele D'Alto <sup>7</sup>, Domenico Filomena<sup>8</sup>, Giovanna Manzi <sup>8</sup>, Antonio Orlando<sup>7</sup>, Alessandra Greco<sup>5</sup>, Tommaso Recchioni<sup>8</sup>, Selin Yildiz<sup>3</sup>, Carmen Jiménez López-Guarch<sup>2</sup>, Alejandro Cruz-Utrilla<sup>2</sup>, Polykarpos Psochias<sup>6</sup>, Vasiliki Patsiou<sup>6</sup>, Jakub Stępniewski<sup>4</sup>, Kamil Jonas<sup>4</sup>, Laura Scelsi<sup>5</sup>, Nils Kremer<sup>3</sup>, Andrea Vergara<sup>7</sup>, Carmine Dario Vizza<sup>8</sup>, Robert Naeije<sup>9</sup>, and Roberto Badagliacca<sup>8,\*</sup>; The ULTRASound RIGHT venTricular eVALUation in pulmonary arterial hypErtension group

<sup>1</sup>National Pulmonary Hypertension Service, Hammersmith Hospital, Imperial College NHS Trust, London, United Kingdom

<sup>2</sup>Multidisciplinary Pulmonary Hypertension Unit, Hospital 12 de Octubre, Madrid, Spain

<sup>3</sup>Department of Internal Medicine, Justus-Liebig-University Giessen, Universities of Giessen and Marburg Lung Center (UGMLC), German Center for Lung Research (DZL), Giessen, Germany

<sup>4</sup>Pulmonary Circulation Centre, Department of Cardiac and Vascular Diseases, Jagiellonian University Medical College, Centre for Rare Cardiovascular Diseases, St. John Paul II Hospital in Krakow, Krakow, Poland

<sup>5</sup>Divisione di Cardiologia, Fondazione IRCCS Policlinico S Matteo, Pavia, Italy

<sup>6</sup>First Cardiology Department, AHEPA Hospital, Aristotle University of Thessaloniki, Thessaloniki, Greece

<sup>7</sup>Department of Cardiology, Monaldi Hospital, Napoli, Italy

<sup>8</sup>Department of Clinical Internal, Anesthesiological and Cardiovascular Sciences, Sapienza University of Rome, Viale del Policlinico 155, Rome 00161, Italy

<sup>9</sup>Department of Pathophysiology, Free University of Brussels, Brussels, Belgium

Received 19 August 2024; accepted after revision 2 November 2024; online publish-ahead-of-print 15 January 2025

## Abstract

### Aims

Outcome in pulmonary arterial hypertension (PAH) is determined by right ventricular (RV) function adaptation to increased afterload. Echocardiography is easily available to assist bedside evaluation of the RV. However, no agreement exists about the feasibility and most relevant measurements. We therefore examined the feasibility, quality, and clinical correlations of standard echocardiographic variables in the evaluation of PAH.

### Methods and results

The present multicentric study collected echocardiographic examinations with centralized reading in 401 patients with prevalent PAH. Clinical variables, as World Health Organization (WHO) functional class (FC), 6 min walk distance (6MWD), brain natriuretic peptide (BNP)/NT-proBNP, invasive haemodynamics, the European Society of Cardiology (ESC)/European Respiratory Society (ERS) guidelines-derived four-strata score, and the United States Registry to Evaluate Early and Long-Term Pulmonary Arterial Hypertension Disease Management (REVEAL) 2.0 score, were also collected. Echocardiographic measurements showed variable degrees of dilation of the right heart as assessed by right atrial and RV areas, altered indices of systolic function such as tricuspid annular plane systolic excursion (TAPSE), fractional area

\* Corresponding author. E-mail: [roberto.badagliacca@uniroma1.it](mailto:roberto.badagliacca@uniroma1.it)

© The Author(s) 2025. Published by Oxford University Press on behalf of the European Society of Cardiology.

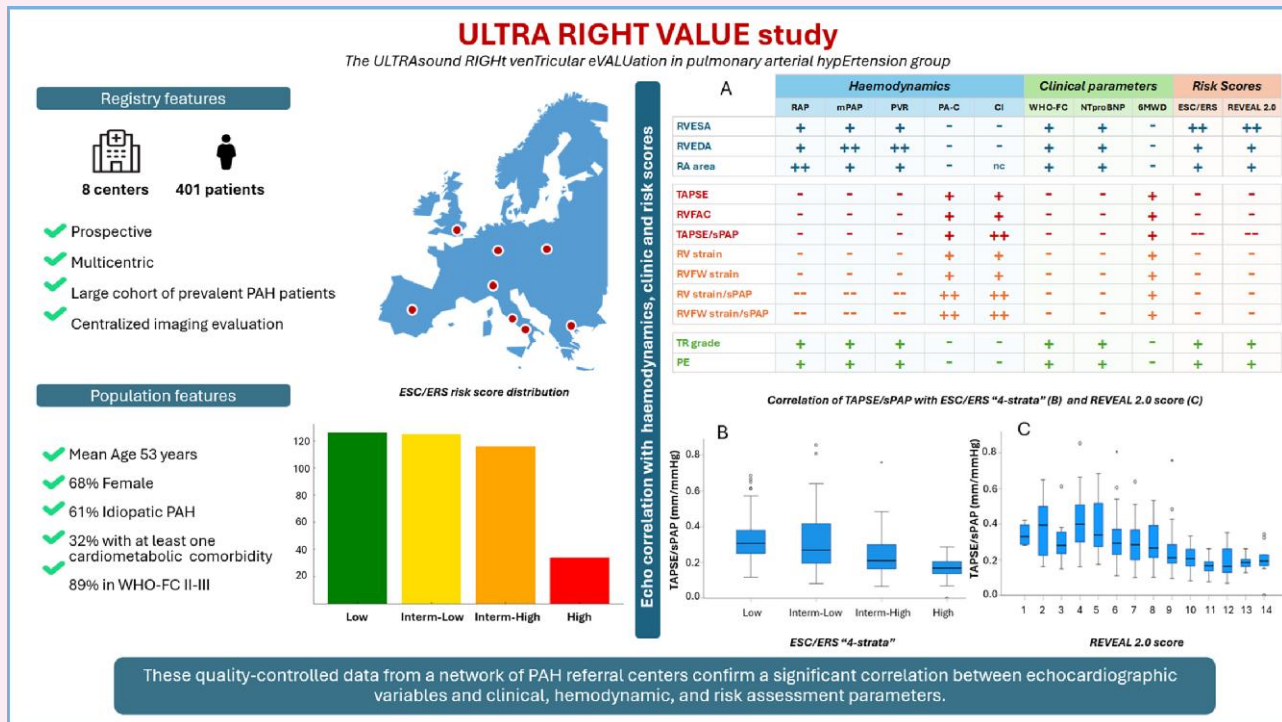
This is an Open Access article distributed under the terms of the Creative Commons Attribution-NonCommercial License (<https://creativecommons.org/licenses/by-nc/4.0/>), which permits non-commercial re-use, distribution, and reproduction in any medium, provided the original work is properly cited. For commercial re-use, please contact [reprints@oup.com](mailto:reprints@oup.com) for reprints and translation rights for reprints. All other permissions can be obtained through our RightsLink service via the Permissions link on the article page on our site—for further information please contact [journals.permissions@oup.com](mailto:journals.permissions@oup.com).

change, or 2D strain, and derived estimates of RV to pulmonary artery (PA) coupling by referring these measurements to systolic PA pressure (sPAP). All these measurements were feasible. All measurements of right heart dimensions and function, particularly TAPSE/sPAP, were correlated with WHO-FC, 6MWD, BNP/NT-proBNP, invasive haemodynamics, and ESC/ERS and REVEAL 2.0 scores.

## Conclusion

The present quality-controlled data from a network of PAH referral centres offer the background needed for further evaluation of the added value of echocardiography to currently recommended risk assessments in PAH.

## Graphical Abstract



6MWD, 6 min walk distance; CI, cardiac index; EDA, end-diastolic area; ERS, European Respiratory Society; ESC, European Society of Cardiology; ESA, end-systolic area; FAC, fractional area change; FW, free wall; mPAP, mean pulmonary artery pressure; NT-proBNP, N-terminal pro b-type natriuretic peptide; PA-C, pulmonary arterial compliance; PAH, pulmonary arterial hypertension; PE, pericardial effusion; PVR, pulmonary vascular resistance; RA, right atrium; RAP, right atrial pressure; REVEAL 2.0, Risk Estimation for Pulmonary Arterial Hypertension 2.0; RV, right ventricle; sPAP, systolic pulmonary artery pressure; TAPSE, tricuspid annular plane systolic excursion; WHO-FC, World Health Organization Functional Class.

## Keywords

pulmonary arterial hypertension • echocardiography • phenotyping • outcome • right heart

## Introduction

Pulmonary arterial hypertension (PAH) is a rare dyspnoea-fatigue syndrome caused by a progressive increase in pulmonary vascular resistance (PVR) and right ventricular (RV) failure<sup>1,2</sup>. In spite of extensive pulmonary vascular remodelling, lung function in these patients is preserved and exercise limitation is determined by the cardiovascular system.<sup>3</sup> Evidence has been accumulated over the last decades that symptoms and outcome in PAH are mainly determined by RV function, yet there is no consensus on how to measure it in daily clinical practice.<sup>1-5</sup>

The RV initially adapts to increased pulmonary artery pressure (PAP) by an enhanced contractility to preserve its coupling to the pulmonary circulation with no or minimal increase in its dimensions. When this 'homeometric' systolic function response gets exhausted, the RV relies on a 'heterometric' increase in dimensions to preserve flow output

matching metabolic demand, at the price of increased filling pressures and eventual systemic congestion.<sup>3-5</sup> Therefore, assessment of the RV in PAH mainly relies on measurements of systolic function and dimensions.

Gold standard measurements of the RV function require invasive conductance catheter technology, which is costly, time-consuming, and not practical at the bedside.<sup>6</sup> Surrogate cardiac magnetic resonance imaging has been developed but this approach is still not widely available or sufficiently feasible in most PAH reference centres.<sup>3-5</sup> Therefore, PAH clinicians rely on simple daily routine echocardiographic examinations, mostly two-dimensional (2D) and complete their clinical assessment with brain natriuretic peptide (BNP) or N-terminal proBNP (NT-proBNP) determinations.

2D echocardiography provides a series of measurements of RV structure and function both at rest and during exercise.<sup>7</sup> While many

of these measurements are included in current guidelines for the diagnosis and treatment of PAH, they have not yet been integrated into the recommended risk scores.<sup>1,2</sup> Several of these measurements have been shown to be of prognostic relevance, but with methodological limitations preventing straightforward integration.<sup>8</sup> Most recently, there has been report on improved United States Registry to Evaluate Early and Long-Term Pulmonary Arterial Hypertension Disease Management (REVEAL) risk score by integration of echocardiographic assessments of RV dimensions, systolic function, tricuspid regurgitation (TR) severity, and pericardial effusion.<sup>9</sup> However, as acknowledged by the authors, this was a retrospective sub-study, also limited by the subjective nature of the echocardiographic assessments. Therefore, there is still an unmet need of a multicentric prospective study with quantitative measurements and a centralized reading of the recordings, thus meeting currently required rigorous methodology.<sup>10,11</sup>

We therefore decided on a feasibility multicentric study for the quantitative evaluation of echocardiographic parameters of the right heart used in clinical practice in relation to haemodynamics, World Health Organization (WHO) functional class (FC), 6 min walk distance (6MWD), NT-proBNP, and risk scores in a large multicentre European prospective cohort of patients with prevalent PAH enrolled in the ULTRASound RIGHt venTricular eVALUation in pulmonary arterial hypertension (ULTRA RIGHT VALUE) study.

## Methods

### Population and study design

We prospectively collected data of consecutively enrolled prevalent patients aged  $\geq 18$  years with idiopathic, heritable, or drug- and toxin-induced PAH, or associated with connective tissue disease, human immunodeficiency virus, portopulmonary hypertension, and corrected-congenital heart disease between January 2022 and December 2023 in eight European referral centres for PAH. The diagnostic work-up and management followed the 2015 European Society of Cardiology (ESC)/European Respiratory Society (ERS) guidelines for patients enrolled up to the end of August 2022<sup>2</sup> and the updated 2022 guidelines thereafter.<sup>1</sup> The haemodynamic definition of pre-capillary pulmonary hypertension was based on the criteria available at the time of enrolment: mean pulmonary artery pressure (mPAP)  $> 25$  mmHg, pulmonary artery wedge pressure (PAWP)  $\leq 15$  mmHg, and PVR  $> 3$  Wood units (WU) until August 2022 and mPAP  $> 20$  mmHg, PAWP  $\leq 15$  mmHg, and PVR  $> 2$  WU thereafter.<sup>1,2</sup> The diagnostic algorithm included also pulmonary function tests, ventilatory and perfusion lung scan, computed tomography of the chest, and echocardiography. All patients enrolled were non-responders to acute vasodilator testing with nitric oxide at the time of diagnosis. Patients had a complete evaluation including WHO functional class, 6MWD, BNP or NT-proBNP, echocardiographic assessment, and right heart catheterization by standard procedures. Risk assessment relied on the ESC/ERS guidelines-derived four-strata model,<sup>12</sup> which incorporates WHO functional class, 6MWD, and BNP/NT-proBNP, and on the REVEAL 2.0 score,<sup>13</sup> which incorporates aetiology, age, sex, WHO-FC, systolic blood pressure, heart rate, right atrial pressure (RAP), PVR, 6MWD, lung diffusing capacity for carbon monoxide, NT-proBNP, renal function, echocardiography, and previous hospitalization.

Treatments were prescribed following contemporary guidelines available at the time of enrolment, according to clinician's decision-making.

The study complied with the Declaration of Helsinki and was approved by the Institutional Review Board for Human Studies of each centre (Protocol n. 638/18 for the Policlinico Umberto I—Sapienza University of Rome, coordinator centre).

### Data collection

All data were captured and stored in electronic case report forms. The investigator and clinical site staff were trained to enter and edit the data via a secure network, with secure access features. The investigator/delegate approved the data using an electronic signature.

All clinical information requested in this protocol were recorded by the investigator or his/her authorized staff in the electronic case report forms in accordance with study-specific data entry rules.

Periodically, a clinical research associate reviewed remotely the accuracy and completeness of all the data entered in the electronic database to ensure quality.

All clinical information were recorded, processed, handled, and stored without disclosing personal information of the subject so that it can be accurately reported, interpreted, and verified while the confidentiality of records and the personal data of the subject remains protected in accordance with the Regulation (EU) 2016/679 (General Data Protection Regulation).

### Echocardiographic core laboratory

All echocardiographic imaging performed into this study were transferred electronically to the echocardiographic core laboratory located in Rome (Department of Clinical, Internal, Anesthesiological, and Cardiovascular Sciences—AOU Policlinico Umberto I, 'Sapienza' University of Rome, Italy). The core laboratory evaluated all standard imaging recordings and interpreted the results.

Each centre was required to perform an echocardiography site accreditation and send echo recordings to the core laboratory. The accreditation procedure ensured the repeatability of acquisition.

Echocardiographic images were stripped of identifiers present within the Digital Imaging and Communication in Medicine (DICOM) header automatically by the electronic software during the imaging upload process.

### Echocardiographic measurements

Measurements were provided through a vendor-independent software solution for cardiac ultrasound by Medis Medical Imaging. Image post-processing tools for advanced cardiac deformation analysis were used for the quantitative evaluation of imaging and for speckle tracking 2D strain assessment.<sup>14,15</sup> This new software allows clinicians to interact with the semi-automatically generated contours of the ventricles for manual editing and review purposes. The introduction of Rubber Banding in QStrain Echo Research Edition optimizes the contour handling, including move-contour and smooth-contour functions.

The following parameters were measured and analysed following US-European guidelines<sup>16,17</sup>: right atrial area (RA area), RV end-diastolic area (RVEDA), RV end-systolic area (RVESA), RV fractional area change % [RVFAC = (RVEDA – RVESA)/RVEDA  $\times$  100], tricuspid annular plane systolic excursion (TAPSE), left ventricular systolic and diastolic eccentricity index (LVELs and LVELd, respectively, defined as the ratio of the anterior–inferior and septal–posterolateral cavity dimensions in short axis, both in systole and diastole), left ventricular end-diastolic area, left ventricular end-systolic area, left ventricular ejection fraction (Simpson method), left atrial area, qualitative assessment of TR, inferior vena cava, estimation of systolic pulmonary arterial pressure (sPAP) from TR velocity, and the presence of pericardial effusion.

Pulsed waved tissue Doppler imaging was used for the measurements of RV isovolumic contraction velocity (IVV), isovolumic acceleration (IVA), and peak systolic velocity (S').

To assess the segmental characteristics of the RV by speckle tracking analysis, we adopted the six-segment RV model. Peak systolic strain amplitude and time intervals from QRS onset to peak systolic strain were calculated for all the RV myocardial segments in the longitudinal direction. RV 2D global strain and RV free wall (FW) 2D basal-mid strain were provided.

Time intervals were corrected for the heart rate according to the Bazett's formula.<sup>18</sup> To quantify RV dyssynchrony, we calculated the standard deviation (SD) of the times to peak systolic strain for the four mid-basal RV segments corrected to the R–R interval between two QRS complexes to derive a so-called RV-SD4.<sup>19,20</sup>

Combined echocardiographic parameters to assess RV–PA coupling<sup>9</sup> were also reported as the ratio between RV systolic functional variables and sPAP: TAPSE/sPAP, RVFAC/sPAP, RV global strain/sPAP, and RVFW basal-mid strain/sPAP. For patients with severe TR, where sPAP was not measurable, the invasive sPAP was used for the ratio calculation.

All reported measurements are the averages derived from three consecutive cardiac cycles.

Limits of normal were derived from the literature.<sup>16,21</sup>

**Table 1** Demographic, clinical, and haemodynamic characteristics of the study population

Patients	401
Age, years	52 ± 17
Female sex, (%)	275 (68%)
Weight, kg	71 ± 16
Height, cm	165 ± 9
BSA, m <sup>2</sup>	1.78 ± 0.22
BMI, kg/m <sup>2</sup>	26 ± 5
Time from diagnosis, months	43 ± 65
PAH classification, n (%)	
Idiopathic	244 (61)
Heritable	31 (8)
Drug/toxin-induced	8 (2)
CTD-SSc	66 (16)
CTD-nonSSc	27 (7)
HIV	8 (2)
Portopulmonary	11 (3)
CHD corrected	6 (1)
Comorbidities, n (%)	
Hypertension	56 (14.0)
Hypercholesterolaemia	28 (7.0)
Coronary artery disease	17 (4.2)
Atrial fibrillation	19 (4.7)
Diabetes	10 (2.5)
N. of comorbidities, n (%)	
0	271 (67.6)
1	114 (28.4)
>1	16 (4.0)
WHO class, n (%)	
I	22 (5.5)
II	179 (44.6)
III	178 (44.4)
IV	22 (5.5)
6MWT, m	355 ± 124
NT-proBNP, pg/mL	362 (140–1243)
Haemodynamics	
Heart rate, b/min	76 ± 12
mPAP, mmHg	45 ± 13
RAP, mmHg	7.3 ± 4.2
CI, L/min/m <sup>2</sup>	2.6 ± 0.8
PWP, mmHg	9.2 ± 3.1
PVR, WU	8.8 ± 5.0
Compliance, mL/mmHg	1.7 ± 1.2
ESC/ERS score, n (%)	
Low	126 (31.4)
Intermediate-low	125 (31.2)
Intermediate-high	116 (28.9)
High	34 (8.5)
REVEAL 2.0 score, n (%)	
1–6	144 (35.9)
7–8	143 (35.7)
9–14	114 (28.4)
Specific therapy, n (%)	

Continued

**Table 1** Continued

ERA/PDE5i monotherapy	94 (23.4)
Double oral combination	134 (33.4)
Triple oral	35 (8.8)
Mono oral + epoprostenol i.v.	9 (2.1)
Mono oral + treprostinil s.c.	6 (1.4)
Double oral + epoprostenol i.v.	40 (10.0)
Double oral + treprostinil s.c.	40 (10.0)
Others	44 (10.9)

6MWT, 6 min walk test; BMI, body mass index; CHD, congenital heart disease; CI, cardiac index; CTD-nonSSc, connective tissue disease; non-systemic sclerosis; CTD-SSc, connective tissue disease; systemic sclerosis; ERA, endothelin receptor antagonist; ESC/ERS, European Society of Cardiology/European Respiratory Society; HIV, human immunodeficiency virus; mPAP, mean pulmonary arterial pressure; NT-proBNP, N-terminal pro b-type natriuretic peptide; PAH, pulmonary arterial hypertension; PDE5i, phosphodiesterase type 5 inhibitor; PVR, pulmonary vascular resistance; PWP, pulmonary wedge pressure; RAP, right atrial pressure; REVEAL 2.0, Registry to Evaluate Early and Long-term PAH Disease Management; WHO, World Health Organization.

## Right heart catheterization

Haemodynamic evaluation was made with standard technique, with assessment of right heart haemodynamics including RAP, mPAP, PVR, cardiac index (CI), and pulmonary arterial compliance (PA-C).

## Statistical analysis

Continuous variables are expressed as mean ± SD or median and inter-quartile range (IQR), and categorical variables are expressed as counts and percentages.

As all echocardiographic images were transferred using a web-based platform and centrally analysed, we had no missing data for the present study.

Pearson's correlation (*r*) was used as a parametric measure of the strength and direction of association between two continuous variables. The Spearman's correlation (*ρ*) was used as a nonparametric measure of the strength and direction of association between two variables measured on at least an ordinal scale. The Kendall's tau-b correlation coefficient (*τ<sub>b</sub>*) was used as a nonparametric measure of the strength and direction of association that exists between two variables measured on an ordinal or continuous scale. Finally, the Somers' delta (Somers' *d*) was used as a nonparametric measure of the strength and direction of association between two categorical variables to distinguish between a dependent and independent variable.

Regression analysis was performed to assess the relations between RV systolic function parameters and PVR.

To compare the statistical significance of the difference between two correlation coefficients, we used the Fisher *r*-to-*z* transformation and calculated the *P*-value based on the resulting *z*-score.

All statistical analyses were performed using SPSS software (version 27.0, IBM) and open source package for R.

## Study organization

This study was sponsored by the Italian Pulmonary Hypertension Network (iPHNET) and supported with an unrestricted grant by Ferrer Internacional SA for site management, site monitoring, and centralized imaging reading (in agreement with Italian Legislative Decree 43 of 17/12/2004, art. 2, subparagraph 6).

## Results

### Patient population

Between January 2022 and December 2023, 401 patients with prevalent PAH were enrolled in the study. As shown in [Table 1](#), median age was 53 years (IQR 38–67) and the majority of the patients was



female (275, 68%) with idiopathic PAH (244, 61%). Most of patients showed a pure PAH physiology, while 130 patients (32.4%) had at least one cardiometabolic comorbidity (Table 1). WHO-FC was II or III in 357 (89%) patients. Patients were evenly distributed across the ESC/ERS risk strata with the exception of a smaller group of high-risk patients (34, 8.5%). The distribution of REVEAL 2.0 risk scores was similar.

The median time from diagnosis to enrolment in the study was 34 months (IQR 14–46).

One hundred sixty-nine patients (42.2%) were treated with double oral therapy (33.4%) or triple oral combination (8.8%), while 95 patients (23.5%) had received a parenteral prostacyclin.

Echocardiographic assessment was acquired  $0 \pm 31$  days (289 patients—72%—within 24 h) after right heart catheterization and before any change in therapies. B-mode 2D echocardiography and speckle tracking echocardiography were feasible in all patients. Pulse tissue Doppler imaging identified IVV in 70% of cases and IVA in 85% of cases. sPAP measurement was feasible in 98% of cases.

Baseline echocardiographic parameters showed variable dilation of the right heart and altered indices of systolic function or RV–PA coupling (Table 2).

## Right heart size and pulmonary haemodynamics

The sizes of the RV and RA were normally distributed, ranging from normal to severely increased, and were linearly related to all invasive pulmonary haemodynamic variables (Table 3). Of note, only the TAPSE/sPAP ratio was always below the normal range of values.

Significant correlations were found among RV areas and invasive pulmonary haemodynamics, including RAP, mPAP, PVR, and PA-C with the higher correlation found for RVESA (mPAP:  $r = 0.37$ ,  $P < 0.001$ ; PVR:  $r = 0.35$ ,  $P < 0.001$ ). We observed an increase of  $0.42 \text{ cm}^2$  in RVEDA ( $y = 24.2 + 0.42 \times x$ ,  $P < 0.001$ ) and  $0.52 \text{ cm}^2$  in RVESA ( $y = 14.4 + 0.52 \times x$ ,  $P < 0.001$ ) for every 1 WU increase in PVR. Figure 1 shows the positive correlation of RVESA with PVR (Figure 1A) and the negative correlation with CI (Figure 1B).

RA area was correlated with RV afterload parameters, including mPAP, PVR, and PA-C, as well as with RV filling pressure, expressed as RAP, which showed the higher correlation ( $\rho = 0.28$ ,  $P < 0.001$ ) (Figure 2). RA area was not correlated to CI ( $\rho = -0.09$ ,  $P = \text{ns}$ ).

As an indirect measure of RV dilation, LVEI in systole and diastole showed a non-normal distribution in the whole population. Both systolic and diastolic LVEI were positively correlated with RAP, mPAP, and PVR, and negatively correlated with CI. LVEIs showed the highest correlation with mPAP and PVR (respectively,  $\rho = 0.42$ ,  $P < 0.001$ ;  $\rho = 0.39$ ,  $P < 0.001$ ).

## Associations between right heart size estimates and WHO-FC, 6MWD, NT-proBNP, and risk scores

Patients with the most dilated RV and RA chambers had a more impaired clinical state and higher risk scores in both the ESC/ERS or the REVEAL 2.0 scoring systems.

RV and RA areas were positively correlated to WHO-FC and NT-proBNP, and negatively to the 6MWD. LVEIs and LVEId were positively correlated to WHO-FC and NT-proBNP. LVEId (not LVEIs) was negatively correlated to the 6MWD.

Area measurements of the RV and the RA for all patients at all ESC/ERS and REVEAL 2.0 scores are shown in Table 3 and Figure 3. Both RV and RA areas were larger with increased risk, whether considering the ESC/ERS or the REVEAL 2.0 risk scores. RVESA showed slightly higher correlation coefficients compared with RVEDA and RA area (ESC/ERS score:  $\tau_b = 0.30$ ,  $P < 0.001$ ; REVEAL 2.0 score:  $\tau_b = 0.31$ ,  $P < 0.001$ ).

**Table 2** Echocardiographic characteristics of the study population

Echocardiographic parameter	Study population	Reference range
LVEDA, $\text{cm}^2$	$27.5 \pm 8.2$	$15.9\text{--}35.5^a$
LVESA, $\text{cm}^2$	$12.2 \pm 4.7$	$8.1\text{--}21.3^a$
LVEF, %	$63.2 \pm 3.4$	$\geq 52$ (M), $\geq 54$ (F) <sup>b</sup>
LVEId	$1.22$ ( $1.06\text{--}1.41$ )	$\leq 1.1^c$
LVEIs	$1.27$ ( $1.15\text{--}1.69$ )	$\leq 1.1^c$
LA area, $\text{cm}^2$	$18.3 \pm 5.4$	$\leq 20^c$
RVEDA, $\text{cm}^2$	$27.5 \pm 8.2$	$\leq 25^c$
RVESA, $\text{cm}^2$	$18.6 \pm 7.4$	$\leq 14^c$
RVFAC, %	$33.8 \pm 9.7$	$\geq 35^c$
RVFAC/sPAP, %/mmHg	$0.46$ ( $0.33; 0.69$ )	NA
TAPSE, mm	$18.3 \pm 4.8$	$\geq 17^b$
TAPSE/sPAP, mm/mmHg	$0.25$ ( $0.18; 0.35$ )	$\geq 0.7^d$
TDI RV IVV, cm/s	$7.9 \pm 3.1$	NA
TDI RV IVA, $\text{cm/s}^2$	$2.4$ ( $1.8\text{--}3.3$ )	$\geq 2.2^c$
TDI RV S', cm/s	$10.3 \pm 2.7$	$\geq 9.5^b$
RV 2D global LS, %	$-18.0 \pm 5.7$	NA
RV global LS/sPAP, %/mmHg	$-0.23$ ( $-0.36; -0.16$ )	NA
RVFW 2D basal-mid LS, %	$-21.0 \pm 6.9$	NA
RVFW basal-mid LS/sPAP, %/mmHg	$-0.32$ ( $-0.47; -0.22$ )	NA
RV Dyssynchrony, ms	$45 \pm 25$	$\leq 18^e$
RA area, $\text{cm}^2$	$23.0 \pm 7.2$	$\leq 18^c$
Tricuspid regurgitation, n (%)		
Mild	302 (75.3)	$< 18^c$
Moderate	90 (22.5)	
Severe	9 (2.2)	
IVC, mm	$19.3 \pm 5.4$	$\leq 21^c$
Pericardial effusion, %	54 (13.5)	Absent <sup>c</sup>

2D, two-dimensional; EDA, end-diastolic area; Eld, end-diastolic eccentricity index; EF, ejection fraction; Els, end-systolic eccentricity index; ESA, end-systolic area; FAC, fractional area change; FW, free wall; IVC, inferior vena cava; IVA, isovolumic acceleration; IVV, isovolumic velocity; LA area, left atrial area; LS, longitudinal strain; LV, left ventricle; RA area, right atrial area; RV, right ventricle; S', systolic wave velocity; sPAP, systolic pulmonary artery pressure; TAPSE, tricuspid annular plane systolic excursion; TDI, tissue Doppler imaging.

<sup>a</sup>Hausmann B, Hach H, Voigt B, Simon R. Echocardiography online quantification of left and right ventricular function by automatic boundary detection: reference values and reproducibility in healthy probands. *Z Kardiol*. 1994 Aug;83(8):556–61.

<sup>b</sup>Lang RM, Badano LP, Mor-Avi V, Afkalo J, Armstrong A, Ernande L, Flachskampf FA, Foster E, Goldstein SA, Kuznetsova T, Lancellotti P, Muraru D, Picard MH, Rietzschel ER, Rudski L, Spencer KT, Tsang W, Voigt JU. Recommendations for cardiac chamber quantification by echocardiography in adults: an update from the American Society of Echocardiography and the European Association of Cardiovascular Imaging. *Eur Heart J Cardiovasc Imaging*. 2015 Mar;16(3):233–70.

<sup>c</sup>Rudski LG, Lai WW, Afkalo J, Hua L, Handschumacher MD, Chandrasekaran K et al. Guidelines for the echocardiographic assessment of the right heart in adults: a report from the American Society of Echocardiography. Endorsed by the European Association of Echocardiography, a registered branch of the European Society of Cardiology, and the Canadian Society of Echocardiography. *J Am Soc Echocardiogr*. 2010;23: 685–713.

<sup>d</sup>Derived from: Ferrara F, Rudski LG, Vriz O, Gargani L, Afkalo J, D'Andrea A, D'Alto M, Marra AM, Aciri E, Stanzola AA, Ghio S, Cittadini A, Naeije R, Bossone E. Physiologic correlates of tricuspid annular plane systolic excursion in 1168 healthy subjects. *Int J Cardiol*. 2016 Nov 15;223:736–743.

<sup>e</sup>Badagliacca R, Reali M, Poscia R, Pezzuto B, Papa S, Mezzapasa M, Nocioni M, Valli G, Giannetta E, Sciomer S, Iacoboni C, Fedele F, Vizza CD. Right Intraventricular Dyssynchrony in Idiopathic, Heritable, and Anorexigen-Induced Pulmonary Arterial Hypertension: Clinical Impact and Reversibility. *JACC Cardiovasc Imaging*. 2015 Jun;8(6):642–52.

**Table 3** Correlation of echocardiographic variables with clinical and haemodynamic data

	WHO	6MWD	NT-proBNP	RAP	mPAP	PVR	PA-C	CI	ESC/ERS	REVEAL 2.0
LVEDA, cm <sup>2</sup>	P < 0.001 r <sub>b</sub> = -0.22	P < 0.001 r = 0.20	P = 0.003 r = -0.25	P = 0.01 r = -0.15	P = 0.007 r = -0.16	P < 0.001 r = -0.30	P < 0.001 r = 0.22	P < 0.001 r = 0.25	P < 0.001 r <sub>b</sub> = -0.27	P < 0.001 r <sub>b</sub> = -0.26
LVEDA-i, cm <sup>2</sup> /m <sup>2</sup>	P < 0.001 r <sub>b</sub> = -0.25	P = 0.005 r = 0.17	P = 0.02 r = -0.19	P = 0.004 r = -0.17	P = ns r = -0.12	P = 0.004 r = -0.17	P = 0.01 r = 0.15	P < 0.001 r = 0.23	P < 0.001 r <sub>b</sub> = -0.29	P < 0.001 r <sub>b</sub> = -0.27
LVESA, cm <sup>2</sup>	P < 0.001 r <sub>b</sub> = -0.17	P = 0.002 r = 0.19	P = 0.002 r = -0.26	P = 0.02 r = -0.14	P < 0.001 r = -0.20	P < 0.001 r = -0.30	P < 0.001 r = 0.26	P < 0.001 r = 0.23	P < 0.001 r <sub>b</sub> = -0.21	P < 0.001 r <sub>b</sub> = -0.20
LVESA-i, cm <sup>2</sup> /m <sup>2</sup>	P < 0.001 r <sub>b</sub> = -0.19	P = 0.005 r = 0.17	P = 0.01 r = -0.21	P = 0.005 r = -0.17	P = 0.005 r = -0.17	P < 0.001 r = -0.21	P = 0.001 r = 0.20	P < 0.001 r = 0.22	P < 0.001 r <sub>b</sub> = -0.21	P < 0.001 r <sub>b</sub> = -0.20
LVEId	P < 0.001 r <sub>b</sub> = 0.19	P = 0.01 r = -0.15	P < 0.001 r = 0.31	P < 0.001 r = 0.20	P < 0.001 r = 0.32	P < 0.001 r = 0.35	P < 0.001 r = -0.23	P < 0.001 r = 0.01	P < 0.001 r <sub>b</sub> = 0.21	P < 0.001 r <sub>b</sub> = 0.23
LVEIs	P < 0.001 r <sub>b</sub> = 0.16	P = ns r = -0.09	P = 0.002 r = 0.26	P = 0.002 r = 0.19	P < 0.001 r = 0.42	P < 0.001 r = 0.39	P < 0.001 r = -0.29	P = 0.01 r = -0.15	P < 0.001 r <sub>b</sub> = 0.17	P < 0.001 r <sub>b</sub> = 0.23
LA area, cm <sup>2</sup>	P < 0.001 r <sub>b</sub> = 0.20	P = ns r = 0.01	P = ns r = 0.04	P = ns r = -0.02	P = 0.008 r = -0.16	P < 0.001 r = -0.28	P = 0.001 r = -0.19	P = 0.003 r = -0.18	P < 0.001 r <sub>b</sub> = 0.28	P < 0.001 r <sub>b</sub> = 0.27
LA area-i, cm <sup>2</sup> /m <sup>2</sup>	P = ns r <sub>b</sub> = -0.06	P = ns r = 0.02	P = ns r = 0.04	P = ns r = -0.05	P = 0.01 r = -0.14	P = 0.002 r = -0.19	P = 0.02 r = 0.14	P < 0.001 r = 0.20	P = ns r <sub>b</sub> = -0.002	P = ns r <sub>b</sub> = -0.03
RA area, cm <sup>2</sup>	P < 0.001 r <sub>b</sub> = 0.20	P < 0.001 r = -0.25	P < 0.001 r = 0.41	P < 0.001 r = 0.28	P < 0.001 r = 0.24	P = 0.01 r = 0.15	P = 0.007 r = -0.16	P = ns r = -0.09	P < 0.001 r <sub>b</sub> = 0.28	P < 0.001 r <sub>b</sub> = 0.27
RA area-i, cm <sup>2</sup> /m <sup>2</sup>	P < 0.001 r <sub>b</sub> = 0.19	P < 0.001 r = -0.22	P < 0.001 r = 0.45	P = 0.003 r = 0.18	P = 0.001 r = 0.19	P < 0.001 r = 0.24	P = 0.01 r = -0.15	P = ns r = -0.08	P < 0.001 r <sub>b</sub> = 0.30	P < 0.001 r <sub>b</sub> = 0.29
RVEDA, cm <sup>2</sup>	P < 0.001 r <sub>b</sub> = 0.22	P = 0.006 r = -0.17	P < 0.001 r = 0.39	P = 0.002 r = 0.19	P < 0.001 r = 0.30	P < 0.001 r = 0.25	P = 0.002 r = -0.12	P = 0.003 r = -0.18	P < 0.001 r <sub>b</sub> = 0.24	P < 0.001 r <sub>b</sub> = 0.26
RVEDA-i, cm <sup>2</sup> /m <sup>2</sup>	P < 0.001 r <sub>b</sub> = 0.22	P = 0.02 r = -0.14	P < 0.001 r = 0.41	P = 0.04 r = 0.12	P < 0.001 r = 0.34	P < 0.001 r = 0.39	P = 0.001 r = -0.19	P = 0.002 r = -0.19	P < 0.001 r <sub>b</sub> = 0.25	P < 0.001 r <sub>b</sub> = 0.28
RVESA, cm <sup>2</sup>	P < 0.001 r <sub>b</sub> = 0.28	P < 0.001 r = -0.23	P < 0.001 r = 0.42	P < 0.001 r = 0.23	P < 0.001 r = 0.37	P < 0.001 r = 0.35	P < 0.001 r = -0.21	P < 0.001 r = -0.26	P < 0.001 r <sub>b</sub> = 0.30	P < 0.001 r <sub>b</sub> = 0.31
RVESA-i, cm <sup>2</sup> /m <sup>2</sup>	P < 0.001 r <sub>b</sub> = 0.28	P < 0.001 r = -0.21	P < 0.001 r = 0.44	P = 0.003 r = 0.18	P < 0.001 r = 0.40	P < 0.001 r = 0.45	P < 0.001 r = -0.27	P < 0.001 r = -0.27	P < 0.001 r <sub>b</sub> = 0.30	P < 0.001 r <sub>b</sub> = 0.31
RVFAC, %	P < 0.001 r <sub>b</sub> = -0.31	P < 0.001 r = 0.30	P < 0.001 r = -0.34	P < 0.001 r = -0.24	P < 0.001 r = -0.43	P < 0.001 r = -0.44	P < 0.001 r = 0.33	P < 0.001 r = -0.34	P < 0.001 r <sub>b</sub> = -0.32	P < 0.001 r <sub>b</sub> = -0.31
RVFAC/sPAP, %/mmHg	P < 0.001 r <sub>b</sub> = -0.29	P < 0.001 r = 0.29	P < 0.001 r = -0.40	P < 0.001 r = -0.31	P < 0.001 r = -0.78	P < 0.001 r = -0.70	P < 0.001 r = 0.71	P < 0.001 r = 0.36	P < 0.001 r <sub>b</sub> = -0.30	P < 0.001 r <sub>b</sub> = -0.33
TAPSE, mm	P < 0.001 r <sub>b</sub> = -0.26	P < 0.001 r = 0.31	P = 0.001 r = -0.28	P < 0.001 r = -0.28	P < 0.001 r = -0.25	P < 0.001 r = -0.38	P < 0.001 r = 0.23	P < 0.001 r = -0.41	P < 0.001 r <sub>b</sub> = -0.29	P < 0.001 r <sub>b</sub> = -0.27
TAPSE/sPAP, mm/mmHg	P < 0.001 r <sub>b</sub> = -0.28	P < 0.001 r = 0.31	P < 0.001 r = -0.39	P < 0.001 r = -0.36	P < 0.001 r = -0.76	P < 0.001 r = -0.73	P < 0.001 r = 0.71	P < 0.001 r = 0.44	P < 0.001 r <sub>b</sub> = -0.30	P < 0.001 r <sub>b</sub> = -0.35
pTDI IVA, m/s <sup>2</sup>	P = ns r <sub>b</sub> = -0.01	P = ns r = 0.004	P = ns r = -0.11	P = ns r = -0.11	P = 0.005 r = -0.20	P = 0.004 r = 0.20	P = 0.003 r = 0.21	P = 0.005 r = 0.20	P = ns r <sub>b</sub> = -0.03	P = ns r <sub>b</sub> = -0.02

Continued

Table 3 Continued

	WHO	6MWD	NT-proBNP	RAP	mPAP	PVR	PA-C	CI	ESC/ERS	REVEAL 2.0
pTDI IVV, cm/s	$P = \text{ns}$ $\tau_b = -0.05$	$P = \text{ns}$ $r = 0.08$	$P = \text{ns}$ $r = -0.15$	$P = 0.006$ $r = -0.19$	$P < 0.001$ $r = -0.36$	$P < 0.001$ $r = -0.32$	$P < 0.001$ $r = 0.27$	$P = 0.04$ $r = 0.14$	$P = \text{ns}$ $\tau_b = -0.06$	$P = \text{ns}$ $\tau_b = -0.08$
pTDI s', cm/s	$P = 0.001$ $\tau_b = -0.15$	$P = 0.03$ $r = 0.15$	$P = 0.005$ $r = -0.27$	$P = 0.004$ $r = -0.19$	$P < 0.001$ $r = -0.24$	$P < 0.001$ $r = -0.36$	$P < 0.001$ $r = 0.24$	$P < 0.001$ $r = 0.31$	$P < 0.001$ $\tau_b = -0.17$	$P < 0.001$ $\tau_b = -0.16$
RV 2D global LS, %	$P < 0.001$ $\tau_b = 0.28$	$P < 0.001$ $r = -0.29$	$P < 0.001$ $r = 0.34$	$P < 0.001$ $r = 0.23$	$P < 0.001$ $r = 0.37$	$P < 0.001$ $r = 0.40$	$P < 0.001$ $r = -0.23$	$P < 0.001$ $r = -0.32$	$P < 0.001$ $\tau_b = 0.31$	$P < 0.001$ $\tau_b = 0.31$
RV 2 global LS/sPAP, %/mmHg	$P < 0.001$ $\tau_b = 0.29$	$P < 0.001$ $\rho = -0.28$	$P < 0.001$ $\rho = 0.39$	$P < 0.001$ $\rho = 0.30$	$P < 0.001$ $\rho = 0.73$	$P < 0.001$ $\rho = 0.69$	$P < 0.001$ $\rho = -0.67$	$P < 0.001$ $\rho = -0.38$	$P < 0.001$ $\tau_b = 0.31$	$P < 0.001$ $\tau_b = 0.34$
RVFW 2D mid-basal LS, %	$P < 0.001$ $\tau_b = 0.30$	$P < 0.001$ $r = -0.29$	$P < 0.001$ $r = 0.38$	$P < 0.001$ $r = 0.21$	$P < 0.001$ $r = 0.32$	$P < 0.001$ $r = 0.34$	$P < 0.001$ $r = -0.21$	$P < 0.001$ $r = -0.27$	$P < 0.001$ $\tau_b = 0.32$	$P < 0.001$ $\tau_b = 0.31$
RVFW 2D mid-basal LS/sPAP, %/mmHg	$P < 0.001$ $\tau_b = 0.30$	$P < 0.001$ $\rho = -0.29$	$P < 0.001$ $\rho = 0.41$	$P < 0.001$ $\rho = 0.32$	$P < 0.001$ $\rho = 0.76$	$P < 0.001$ $\rho = 0.69$	$P < 0.001$ $\rho = -0.69$	$P < 0.001$ $\rho = -0.36$	$P < 0.001$ $\tau_b = 0.31$	$P < 0.001$ $\tau_b = 0.31$
RV dyssynchrony, ms	$P = 0.006$ $\tau_b = 0.12$	$P = 0.02$ $r = -0.14$	$P = 0.002$ $r = 0.24$	$P = 0.02$ $r = 0.14$	$P = 0.03$ $r = 0.13$	$P = 0.001$ $r = 0.20$	$P = \text{ns}$ $r = -0.03$	$P = 0.002$ $r = -0.19$	$P < 0.001$ $\tau_b = 0.14$	$P = 0.002$ $\tau_b = 0.13$
Pericardial effusion	$P = 0.001$ $d = 0.24$	$P = 0.002$ $\tau_b = -0.16$	$P = \text{ns}$ $\tau_b = 0.11$	$P = 0.03$ $\tau_b = 0.11$	$P = 0.01$ $\tau_b = 0.12$	$P = 0.01$ $\tau_b = 0.13$	$P = 0.03$ $\tau_b = -0.11$	$P = 0.03$ $\tau_b = -0.10$	$P < 0.001$ $d = 0.19$	$P < 0.001$ $d = 0.33$
Tricuspid reg, grade	$P = 0.002$ $d = 0.14$	$P < 0.001$ $\tau_b = -0.25$	$P < 0.001$ $\tau_b = -0.26$	$P = 0.003$ $\tau_b = 0.14$	$P = 0.02$ $\tau_b = 0.11$	$P < 0.001$ $\tau_b = 0.15$	$P = 0.001$ $\tau_b = -0.15$	$P = 0.001$ $\tau_b = -0.15$	$P < 0.001$ $d = 0.25$	$P < 0.001$ $d = 0.38$

$r$  = Pearson's  $r$  correlation coefficient;  $\tau_b$  = Kendall's tau-b correlation coefficient;  $\rho$  = Spearman rank-order correlation coefficient;  $d$  = Somers' delta correlation coefficient.  
 2D, two-dimensional; 6MWD, 6 min walk distance; -1, indexed to body surface area; CI, cardiac index; ESC/ERS, European Society of Cardiology/European Respiratory Society; EDA, end-diastolic area; Eld, end-diastolic eccentricity index; EF, ejection fraction; Els, end-systolic eccentricity index; ESA, end-systolic area; FAC, fractional area change; FW, free wall; IVC, inferior vena cava; IVA, isovolumic acceleration; IVV, isovolumic velocity; LA area, left atrial area; LS, longitudinal strain; LV, left ventricle; NT-proBNP, N-terminal pro b-type natriuretic peptide; PA-C, pulmonary artery compliance; PVR, pulmonary vascular resistance; RA area, right atrial area; RAP, right atrial pressure; REVEAL 2.0, Registry to Evaluate Early and Long-term PAH Disease Management 2.0; RV, right ventricle; S', systolic wave velocity; sPAP, systolic pulmonary artery pressure; TAPSE, tricuspid annular plane systolic excursion; TDI, tissue Doppler imaging; WHO, World Health Organization.

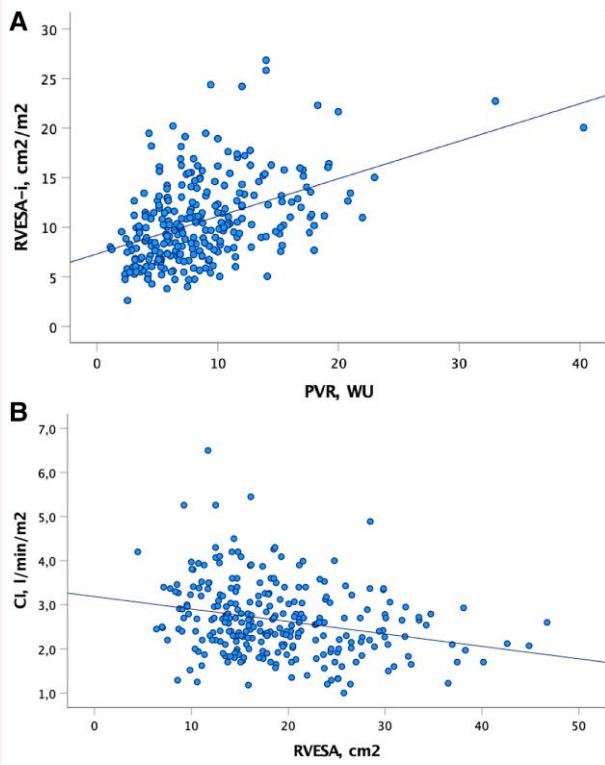


**Figure 1** Correlation of RVESA with PVR (A) and CI (B). The plot shows a positive correlation between RVESA and PVR ( $r = 0.35$ ,  $P < 0.001$ ) (A); a negative correlation with CI ( $r = -0.27$ ,  $P < 0.001$ ) (B). RVESA, right ventricular end-systolic area; PVR, pulmonary vascular resistance; CI, cardiac index.

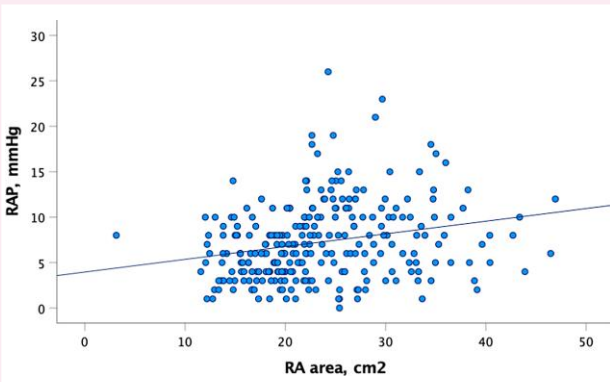


**Figure 2** Correlation of RA area with RAP. The plot shows significant positive correlation between RA pressure and area ( $r = 0.28$ ,  $P < 0.001$ ). RA, right atrium; RAP, right atrial pressure.

Of note, normalization of ventricular and atrial areas for body surface area improved the correlation between RVEDA and RVESA, with PVR, PA-C and mPAP, without affecting others correlations (Table 3).

Finally, when corrected for the severity of TR, the correlation between echocardiographic-derived right heart measurements and

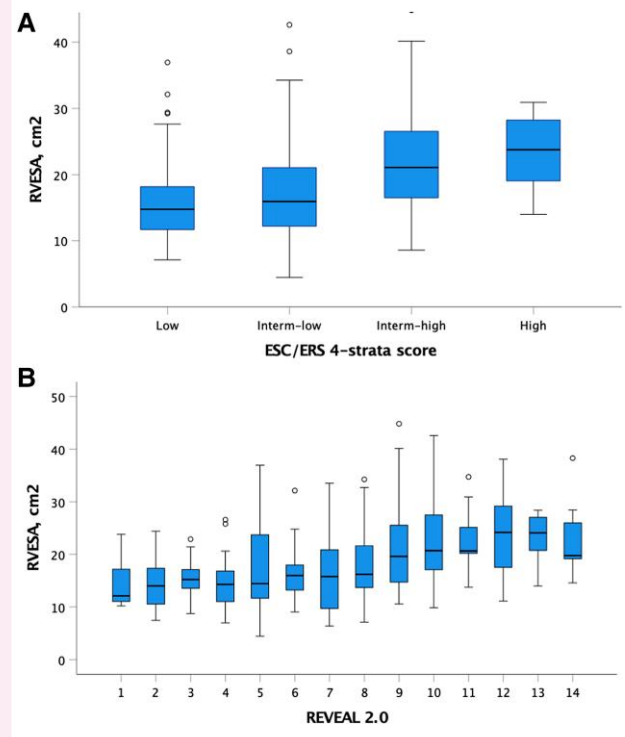


**Figure 3** Box-and-whisker plots showing the distribution of RVESA according to the ESC/ERS 'four-strata' (A) and REVEAL 2.0 (B). RVESA showed significant correlation with ESC/ERS and the REVEAL 2.0 risk score (ESC/ERS score:  $\tau_b = 0.30$ ,  $P < 0.001$ ; REVEAL 2.0 score:  $\tau_b = 0.31$ ,  $P < 0.001$ ). RVESA, right ventricular end-systolic area; ESC, European Society of Cardiology; REVEAL 2.0, United States Registry to Evaluate Early and Long-Term Pulmonary Arterial Hypertension Disease Management.

clinical variables, haemodynamics and risk scores did not improve meaningfully (see [Supplementary data online, Table S1](#)).

## Right ventricular function correlation with pulmonary haemodynamics and risk scores

Both TAPSE and RVFAC were correlated with invasive pulmonary haemodynamics. The RVFAC showed a greater negative correlation with PVR and mPAP, and a positive correlation with PA-C, compared with TAPSE (Table 3; Figure 4). Conversely, TAPSE showed a better negative correlation with CI compared with RVFAC (respectively,  $r = -0.41$ ,  $P < 0.001$ , and  $r = -0.34$ ,  $P < 0.001$ ; TAPSE vs. RVFAC  $P = 0.04$ ), even when corrected for sPAP (respectively,  $r = -0.44$ ,  $P < 0.001$ , and  $r = -0.36$ ,  $P < 0.001$ ; TAPSE/sPAP vs. RVFAC/sPAP  $P = 0.02$ ). Differences in correlation coefficients between TAPSE and RVFAC for PVR, mPAP, and PA-C decreased when variables were corrected for sPAP, further improving the correlation from moderate to strong (Figure 5).

Similar correlation coefficients were observed between TAPSE and RVFAC for RAP distribution.

TAPSE and RVFAC were negatively correlated with WHO-FC and NT-proBNP, and positively correlated with the 6MWD. Both systolic function parameters were negatively associated with ESC/ERS and REVEAL 2.0 risk scores (Figure 6). Correction of both TAPSE and



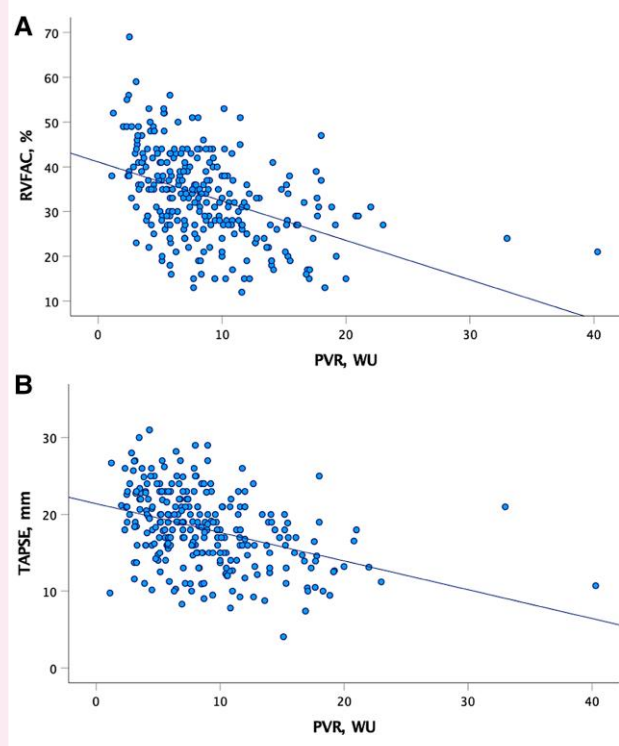


**Figure 4** Correlation of PVR with RVFAC (A) and TAPSE (B). Both RVFAC and TAPSE showed a negative correlation with PVR, greater with RVFAC (respectively,  $r = -0.44$ ,  $P < 0.001$ ;  $r = -0.30$ ,  $P < 0.001$ ). RVFAC, right ventricular fraction area change; TAPSE, tricuspid annular plane systolic excursion; PVR, pulmonary vascular resistance.

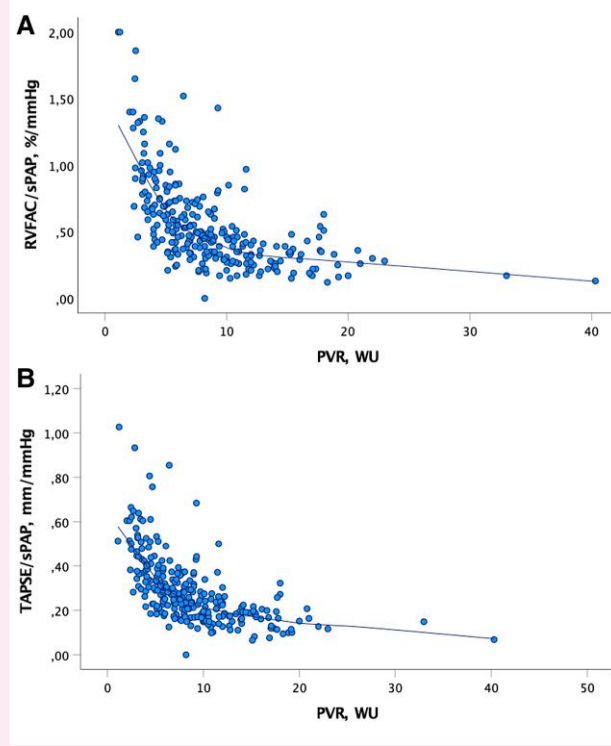


**Figure 5** Correlation of RVFAC/sPAP (A) and TAPSE/sPAP (B) with PVR. Both RVFAC/sPAP and TAPSE/sPAP showed negative correlation with PVR (respectively,  $r = -0.70$ ,  $P < 0.001$ , and  $r = -0.73$ ,  $P < 0.001$ ). RVFAC, right ventricular fraction area change; TAPSE, tricuspid annular plane systolic excursion; sPAP, systolic pulmonary arterial pressure; PVR, pulmonary vascular resistance.

RVFAC for sPAP did not improve substantially the correlation with clinical variables, except for the TAPSE/sPAP with the ESC/ERS and REVEAL 2.0 risk scores (Figure 7).

IVV and IVA showed similar association with pulmonary haemodynamics, presenting positive correlation with RAP, PVR, and mPAP, and negative correlation with PA-C. A higher correlation was observed between IVA and CI, compared with IVV (respectively,  $r = 0.31$ ,  $P < 0.001$ ;  $r = 0.14$ ,  $P = 0.04$ ). IVV was not correlated with clinical variables and risk scores. IVA was weakly correlated to clinical variables, as WHO-FC, 6MWD, NT-proBNP, and risk scores.

Both global RV strain and RVFW strain (excluding the apical segment) were correlated with invasive pulmonary haemodynamics. Both global RV strain and RVFW strain were positively correlated with RAP, PVR, and mPAP, and negatively with PA-C and CI. Similar correlations characterized the association of both global RV strain and RVFW strain with WHO-FC, 6MWD, NT-proBNP, and risk scores. Of note, when the RV dilates, global RV strain is characterized by progressively reduced values compared with the RVFW strain of the basal and middle segments (Figure 8).

Correction for sPAP did not improve the correlation between RV strain, whether global or free wall strain, and clinical variables and risk scores, but improved the correlation with all the invasive haemodynamic variables (Table 3).

Of note, all RV systolic function variables showed similar clinical and haemodynamic correlations once corrected for sPAP, except for TAPSE/sPAP that presented the highest correlation with CI.

The relationship between RV systolic parameters—specifically RVFAC, RV free wall strain, and TAPSE—and PVR had a flatter slope

in severely dilated RVs compared with mildly dilated ones. In cases of mild RV dilation, RVFAC and free wall strain showed a greater percentage decrease per unit increase in PVR compared with TAPSE, with reductions of 1.1%, 0.69%, and 0.46% per 1 PVR WU, respectively ( $P < 0.01$ ) (Figure 9).

Finally, when adjusted for the severity of TR, the correlation between echocardiographic-derived RV systolic function measurements and clinical variables, haemodynamics, and risk scores did not improve meaningfully (see Supplementary data online, Table S1).

Right intraventricular dyssynchrony, calculated as RV-SD4, showed a significant correlation with the invasive haemodynamic variables, except for the PA-C, the WHO-FC, the NT-proBNP, and the ESC/ERS and REVEAL 2.0 risk scores. RV-SD4 was negatively correlated with 6MWD and CI.

## TR and pericardial effusion

There was a positive correlation between the severity of the disease expressed by the ESC/ERS and the REVEAL 2.0 scores and the grade of TR (Table 3). However, the correlation of TR with each relevant component of the scores, as WHO-FC, 6MWD, and NT-proBNP, was weak. A very weak correlation, albeit significant, also characterized the association between invasive pulmonary haemodynamic and tricuspid regurgitation grade.

A significant but weak correlation was found between pericardial effusion and all clinical and haemodynamic variables, including the association with risk scores, whether the ESC/ERS or the REVEAL 2.0.

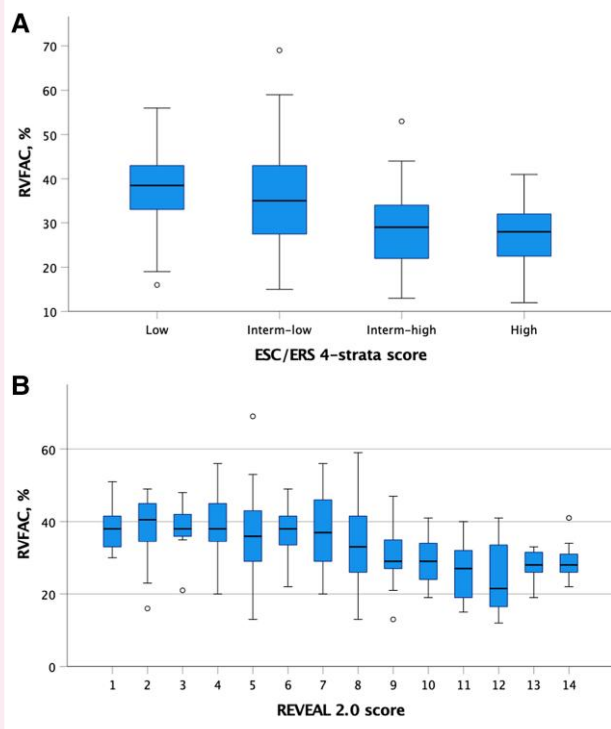


**Figure 6** Box-and-whisker plots showing the distribution of RVFAC according to the ESC/ERS ‘four-strata’ (A) and REVEAL 2.0 (B). Lower RVFAC was associated with higher risk using both ESC/ERS or REVEAL 2.0 risk scores (ESC/ERS score:  $\tau_b = -0.32$ ,  $P < 0.001$ ; REVEAL 2.0 score:  $\tau_b = -0.31$ ,  $P < 0.001$ ). Legend: see previous figures.

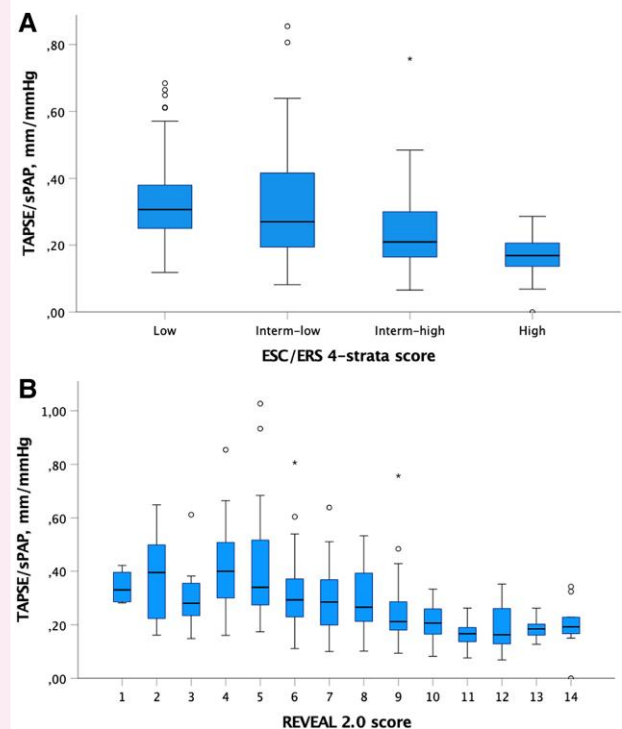


**Figure 7** Box-and-whisker plots showing the distribution of TAPSE/sPAP according to the ESC/ERS ‘four-strata’ (A) and REVEAL 2.0 (B). TAPSE corrected for sPAP correlated with both the ESC/ERS and REVEAL 2.0 risk scores (ESC/ERS score:  $\tau_b = -0.30$ ,  $P < 0.001$ ; REVEAL 2.0 score:  $\tau_b = -0.35$ ,  $P < 0.001$ ). Legend: see previous figures.

## Discussion

The present results, derived from a large multicentric collaboration with central core laboratory quality control, show that standard 2D echocardiographic assessments in PAH are related to disease severity (*Graphical Abstract*). Measurements of right heart dimensions and of RV systolic function combined with sPAP, as a measure of RV–PA coupling, were all correlated to haemodynamic severity and ESC/ERS and REVEAL risk scores, indirectly suggesting prognostic relevance. Echocardiography of the right heart was successfully performed across all eight participating centres, showing excellent feasibility of all relevant variables, except for IVV and IVA measurements.

This is the first European experience of centralized echocardiography reading from multiple referral PAH centres with high quality data-imaging collection, in accordance with imaging process standards by the U.S. Department of Health and Human Services and the Center for Biologics Evaluation and Research (U.S. Department of Health and Human Services Food and Drug Administration Center for Drug Evaluation and Research Center for Biologics Evaluation and Research).<sup>10</sup>

Echocardiography in PAH generates a large number of variables, raising the question of which provide sufficient diagnostic and prognostic information in clinical practice. Redundant measurements may serve as internal controls, but are time-consuming and typically omitted in daily routine. The present study cannot answer the question of an ideal shortened list of the most relevant variables, as sequential correlation calculations only allow for a disqualification of non-significant ones,

which were actually few. A hierarchy of correlation coefficients would be confused by a multiplicity problem, which can only be incompletely resolved with corrections for multiple comparisons. On the other hand, selecting independent predictors of risk scores by a uni/multivariable analysis could not be attempted in the present study because of the overwhelmingly large number of variables. Until prognostic analysis becomes available, it may be preferable to use echocardiographic variables in the framework of the previously discussed physiology of right heart structure and function adaptation to increased afterload in PAH.<sup>3–5</sup> In this respect, assessments of RV remodelling—mainly right atrial and ventricular areas, as well as the left ventricular eccentricity index, as highlighted in studies examining the RV response to drugs that effectively and significantly reduce PVR and improve prognosis<sup>22–24</sup>—are standard approach in daily clinical practice.<sup>25</sup>

Another important aspect is the evaluation of the coupling of RV systolic function to afterload.<sup>5</sup> The present results seem to support the TAPSE/sPAP ratio as the preferred variable compared with FAC/sPAP or strain/sPAP to assess the gold standard ratio of RV end-systolic elastance to pulmonary arterial elastance and predict outcome.<sup>26</sup>

Interestingly, the slope of the relation between RV systolic function parameters and PVR was flatter for TAPSE in mildly dilated RVs compared with RVFAC and RVFW 2D strain, suggesting that the latter are more sensitive to detect disease progression-related changes in RV systolic function in the early stages of the disease.

Global RV strain was characterized by progressively reduced values compared with the RVFW strain of the basal and middle segments. This

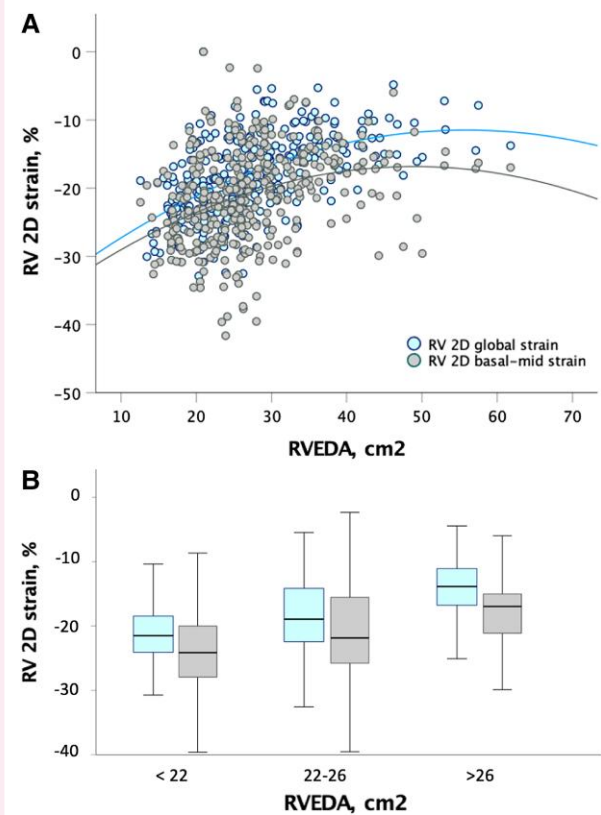


**Figure 8** Correlation between RVEDA and global RV strain and RVFW strain. RV dilatation is associated with progressive reduction of the global RV strain and RVFW strain of the basal and middle segments. (A) Scatterplot of RV 2D strain vs. RVEDA, based on RV global strain measurements and RVFW strain of the basal and middle segments. (B) RV 2D strain median value, based on RV global strain measurements and RVFW strain of the basal and middle segments, vs. tertiles of RVEDA values (<22 cm<sup>2</sup>; 22–26 cm<sup>2</sup>; >26 cm<sup>2</sup>). Box edges represent the 25th (Q1) and 75th (Q3) quartiles, respectively. The upper whisker is drawn at the greatest value smaller than 1.5 IQR above the third quartile, while the lower whisker is drawn at the smallest value > 1.5 IQR below the first quartile. RVEDA, right ventricular end-diastolic area; RV 2D strain, right ventricular two-dimensional strain; RVFW, right ventricular free wall; IQR, interquartile range.

is probably related to technical issues affecting apical segment strain measurement. Indeed, high variability and reduced values characterize RV apical strain, even in normal subjects and especially in dilated RV chambers. This is supported by software-related technical issues,<sup>27</sup> as the measurements are dependent on cavity curvature and region of interest (ROI) width. Thus, because the apparent curvature and the ROI width/myocardial thickness discrepancy are highest in the apex, especially in dilated RV, measurements in apical RV segments are less reliable and characterized by high variability and reduced values.<sup>19,20</sup> The weak correlation of pericardial effusion and TR severity with RAP may be explained by the diuretic regimen optimized for prevalent patients. Greater correlations have been previously described for incident patients.

There has been most recently report of a REVEAL-ECHO risk score by integration of echocardiographic RV dimensions, systolic function, TR severity, and pericardial effusion assessments.<sup>9</sup> The study was limited by its retrospective nature and reliance on qualitative

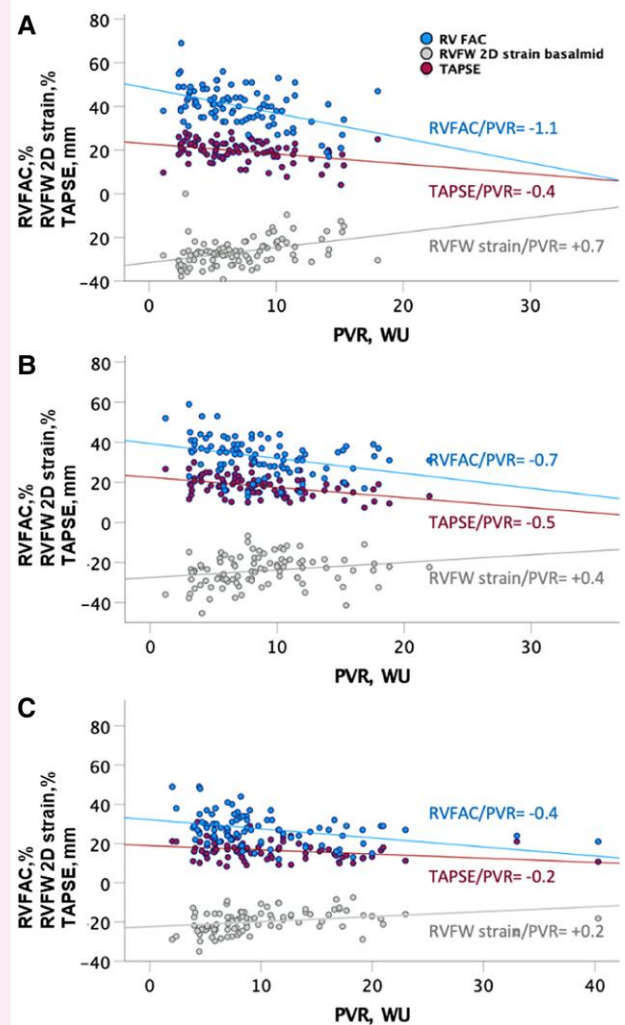


**Figure 9** Correlation between PVR and RV systolic function variables based on RV dilation. The relationship between RV systolic parameters, such as RVFAC, RVFW strain, and TAPSE, and PVR appears flatter when the RV is severely dilated. (A) RVFAC, RVFW strain, and TAPSE, vs. PVR in mildly dilated RVs (RVEDA lower tertile, <22 cm<sup>2</sup>) (respectively, −1.1% per 1 PVR WU; 0.69% per 1 PVR WU; −0.46% per 1 PVR WU,  $P < 0.01$ ); (B) RVFAC, RVFW strain, and TAPSE, vs. PVR in moderately dilated RVs (RVEDA intermediate tertile, 22–26 cm<sup>2</sup>) (respectively, −0.7% per 1 PVR WU; 0.4% per 1 PVR WU; −0.5% per 1 PVR WU,  $P < 0.01$ ); (C) RVFAC, RVFW strain, and TAPSE, vs. PVR in severely dilated RVs (RVEDA higher tertile, >26 cm<sup>2</sup>) (respectively, −0.4% per 1 PVR WU; 0.2% per 1 PVR WU; −0.2% per 1 PVR WU,  $P < 0.01$ ). Legend: see previous figures.

echocardiography, but it demonstrated added value to the REVEAL 2.0 risk score, confirming previous but more limited size studies.<sup>23,28</sup>

## Limitations

The authors acknowledge some limitations in the present study. First, the update of the ESC/ERS guidelines in August 2022 introduced minor

differences in patient management before and after that date. Secondly, for a minority of patients, calculating sPAP via echocardiography was not feasible, so invasive sPAP measurements were used for assessing RV–PA coupling. Thirdly, a sensitivity analysis on the correlation of pericardial effusion with pulmonary haemodynamics for patients with idiopathic, heritable, and toxin-induced PAH was not possible because of the limited number of patients with pericardial effusion (36 out of 283).

## Conclusions

The present findings confirm previously reported relationships between echocardiographic and pulmonary haemodynamic measurements in smaller, mostly mono-centric, mixed origin pulmonary hypertension populations and extend our knowledge on how different stages of right heart impairment affect clinical condition and risk scores assessment. The results may be important for future development of risk scores with integration of imaging of RV structure and function.

## Supplementary data

Supplementary data are available at *European Heart Journal – Imaging Methods and Practice* online.

## Acknowledgements

The authors thank Eduardo Bossone and Francesco Ferrara for deriving the TAPSE/SPAP reference limit from the study cohort of the study by Ferrara et al.<sup>21</sup>

**Consent:** Informed consent was obtained for all participants.

**Funding:** The study was supported with an unrestricted grant by Ferrer Internacional SA for site management, site monitoring, and centralized imaging reading.

**Conflict of interest:** C.D.V. reports personal fees from GSK, UT, Dompè, Bayer, and MSD, outside the submitted work. R.B. reports personal fees from UT, Dompè, Ferrer, Bayer, MSD, AOP Orphan Pharmaceuticals, and Gossamer Bio, outside the submitted work. M.D. reports personal fees from Bayer, Dompè, GSK, MSD, and Ferrer, outside the submitted work. F.L.G. reports fees from Johnson & Johnson, Acthelion, and GSK, not related to the submitted work. R.N. reports personal fees from UT, Lung Biotechnology, Johnson & Johnson, Acthelion, and AOP Orphan Pharmaceuticals, outside the submitted work. G.K. reports personal fees from Jansen, Penumbra, MSD, Bayer, Pfizer, and AOP Orphan, outside the submitted work. J.S. reports personal fees from Jansen, Boston, Penumbra, and MSD, outside the submitted work. K.J. reports personal fees from Jansen, and MSD, outside the submitted work. Other authors have nothing to disclose.

## Lead author biography



Roberto Badagliacca is an Associate Professor of Cardiology at Sapienza University of Rome and the Chief of the Pulmonary Hypertension Program. His research focuses on the pathophysiology, imaging phenotyping, and risk stratification of pulmonary arterial hypertension. He is also the Chairman-Elect of the ESC Working Group on Pulmonary Circulation & Right Ventricular Function.

## References

- Humbert M, Kovacs G, Hoeper MM, Badagliacca R, Berger RMF, Brida M et al. 2022 ESC/ERS guidelines for the diagnosis and treatment of pulmonary hypertension. *Eur Heart J* 2022;**43**:3618–731.
- Galiè N, Humbert M, Vachiery JL, Gibbs S, Lang I, Torbicki A et al. 2015 ESC/ERS guidelines for the diagnosis and treatment of pulmonary hypertension: the joint task force for the diagnosis and treatment of pulmonary hypertension of the European Society of Cardiology (ESC) and the European Respiratory Society (ERS): endorsed by: Association for European Paediatric and Congenital Cardiology (AEPC), International Society for Heart and Lung Transplantation (ISHLT). *Eur Heart J* 2016;**37**:67–119.
- Naeije R, Richter MJ, Rubin LJ. The physiological basis of pulmonary arterial hypertension. *Eur Respir J* 2022;**59**(6):2102334.
- Noordegraaf AV, Chin KM, Haddad F, Hassoun PM, Hemnes AR, Hopkins SR et al. Pathophysiology of the right ventricle and of the pulmonary circulation in pulmonary hypertension: an update. *Eur Respir J* 2019;**53**(1):1801900.
- Tello K, Naeije R, De Man F, Guazzi M. Pathophysiology of the right ventricle in health and disease: an update. *Cardiovasc Res* 2023;**119**:1891–904.
- Brener MI, Lurz P, Hausleiter J, Rodés-Cabau J, Fam N, Kodali SK et al. Right ventricular–pulmonary arterial coupling and afterload reserve in patients undergoing transcatheter tricuspid valve repair. *J Am Coll Cardiol* 2022;**79**:448–61.
- Gargani L, Pugliese NR, De Biase N, Mazzola M, Agoston G, Arcopinto M et al. Exercise stress echocardiography of the right ventricle and pulmonary circulation. *J Am Coll Cardiol* 2023;**82**:1973–85.
- Naeije R. Assessment of right ventricular function in pulmonary hypertension. *Curr Hypertens Rep* 2015;**17**:35.
- El-Kersh K, Zhao C, Elliott G, Farber HW, Gombert-Maitland M, Selej M et al. Derivation of a risk score (REVEAL-ECHO) based on echocardiographic parameters of patients with pulmonary arterial hypertension. *Chest* 2023;**163**:1232–44.
- The U.S. Department of Health and Human Services (Food and Drug Administration) and the Center for Biologics Evaluation and Research (U.S. Department of Health and Human Services Food and Drug Administration Center for Drug Evaluation and Research (CDER) Center for Biologics Evaluation and Research (CBER). The clinical trial imaging endpoint process standards. April 2018. <https://www.fda.gov/Drugs/GuidanceComplianceRegulatoryInformation/Guidances/default.htm>. [Internet] (01 April 2024, date last accessed).
- Atkinson AJ, Colburn WA, DeGruttola VG, DeMets DL, Downing GJ, Hoth DF et al. Biomarkers and surrogate endpoints: preferred definitions and conceptual framework. *Clin Pharmacol Ther* 2001;**69**:89–95.
- Hoeper MM, Pausch C, Olsson KM, Huscher D, Pittrow D, Grünig E et al. COMPERA 2.0: a refined four-stratum risk assessment model for pulmonary arterial hypertension. *Eur Respir J* 2022;**60**:2102311.
- Benza RL, Miller DP, Gombert-Maitland M, Frantz RP, Foreman AJ, Coffey CS et al. Predicting survival in pulmonary arterial hypertension: insights from the Registry to Evaluate Early and Long-Term Pulmonary Arterial Hypertension Disease Management (REVEAL). *Circulation* 2010;**122**:164–72.
- Muraru D, Haugaa K, Donal E, Stankovic I, Voigt JU, Petersen SE et al. Right ventricular longitudinal strain in the clinical routine: a state-of-the-art review. *Eur Heart J Cardiovasc Imaging* 2022;**23**:898–912.
- Badano LP, Kolas TJ, Muraru D, Abraham TP, Aurigemma G, Edvardsen T et al. Standardization of left atrial, right ventricular, and right atrial deformation imaging using two-dimensional speckle tracking echocardiography: a consensus document of the EACVI/ASE/Industry Task Force to standardize deformation imaging. *Eur Heart J Cardiovasc Imaging* 2018;**19**:591–600.
- Rudski LG, Lai WW, Afalalo J, Hua L, Handschumacher MD, Chandrasekaran K et al. Guidelines for the echocardiographic assessment of the right heart in adults: a report from the American Society of Echocardiography endorsed by the European Association of Echocardiography, a registered branch of the European Society of Cardiology, and the Canadian Society of Echocardiography. *J Am Soc Echocardiogr* 2010;**23**:685–713.
- Lang RM, Badano LP, Mor-Avi V, Afalalo J, Armstrong A, Ernande L et al. Recommendations for cardiac chamber quantification by echocardiography in adults: an update from the American Society of Echocardiography and the European Association of Cardiovascular Imaging. *Eur Heart J Cardiovasc Imaging* 2015;**16**:233–71.
- Bazett H. An analysis of the time-relations of electrocardiograms. *Heart* 1920;**7**:353–70.
- Badagliacca R, Reali M, Poscia R, Pezzuto B, Papa S, Mezzapesa M et al. Right intraventricular dyssynchrony in idiopathic, heritable, and anorexigen-induced pulmonary arterial hypertension: clinical impact and reversibility. *JACC Cardiovasc Imaging* 2015;**8**:642–52.
- Badagliacca R, Poscia R, Pezzuto B, Papa S, Gambardella C, Franccone M et al. Right ventricular dyssynchrony in idiopathic pulmonary arterial hypertension: determinants and impact on pump function. *J Heart Lung Transplant* 2015;**34**:381–9.
- Ferrara F, Rudski LG, Vriz O, Gargani L, Afalalo J, D'Andrea A et al. Physiologic correlates of tricuspid annular plane systolic excursion in 1168 healthy subjects. *Int J Cardiol* 2016;**223**:736–43.
- Badagliacca R, Raina A, Ghio S, D'Alto M, Confalonieri M, Correale M et al. Influence of various therapeutic strategies on right ventricular morphology, function and hemodynamics in pulmonary arterial hypertension. *J Heart Lung Transplant* 2018;**37**:365–75.



23. Badagliacca R, Papa S, Manzi G, Miotti C, Luongo F, Sciomer S et al. Usefulness of adding echocardiography of the right heart to risk-assessment scores in prostanoïd-treated pulmonary arterial hypertension. *JACC Cardiovasc Imaging* 2020;**13**:2054–6.
24. D'Alto M, Badagliacca R, Argiento P, Romeo E, Farro A, Papa S et al. Risk reduction and right heart reverse remodeling by upfront triple combination therapy in pulmonary arterial hypertension. *Chest* 2020;**157**:376–83.
25. Rubin LJ, Naeije R. Sotatercept for pulmonary arterial hypertension: something old and something new. *Eur Respir J* 2023;**61**(1):2201972.
26. Tello K, Axmann J, Ghofrani HA, Naeije R, Narcin N, Rieth A et al. Relevance of the TAPSE/PASP ratio in pulmonary arterial hypertension. *Int J Cardiol* 2018;**266**:229–35.
27. NTNU-Trondheim Norwegian University of Science and Technology Strain rate imaging. <https://stoylen.folk.ntnu.no/strainrate/index.html>. (01 April 2024, date last accessed). [Internet]
28. Badagliacca R, Ghio S, D'Alto M, Ameri P, Correale M, Filomena D et al. Relevance of echocardiography-derived phenotyping in patients with pulmonary arterial hypertension treated with initial oral combination therapy: an Italian pulmonary hypertension network (IPHNET) study. *Am J Respir Crit Care Med* 2024;**210**:362–5.